Presented as late breaking results contribution
21st IFAC World Congress (Virtual)
Berlin, Germany, July 12-17, 2020

Consistency analysis of the extended observability matrix of output-error closed-loop subspace model identification ⋆

Hiroshi Oku * **Kenji Ikeda** **

* *Osaka Institute of Technology, Osaka, 535-8585 Japan (e-mail: hiroshi.oku@oit.ac.jp)*
** *Tokushima University, Tokushima, 770-8506 Japan (e-mail: ikeda@is.tokushima-u.ac.jp)*

Abstract: This paper studies statistical properties of a closed-loop subspace model identification method for a system described with the output-error state-space representation. For details, the limit value of the matrix to be singular-value-decomposed to estimate the extended observability matrix is investigated. The contribution is to ensure that the estimate of the extended observability matrix is consistent up to a similarity transform.

Keywords: System identification, closed loop identification, subspace methods, consistency, asymptotic properties.

1. INTRODUCTION

In the early 2000s, closed-loop subspace model identification methods have been proposed and their statistical properties have been studied intensively (e.g. Chiuso and Picci, 2005; Chiuso, 2006, 2010). The focus has mainly been on the so-called direct methods based on prediction-error framework.

Oku et al. (2006a,b) have proposed a closed-loop subspace model identification method for a system described with the output-error state-space representation. Since its procedure resembles that of the "MOESP" family (e.g. Verhaegen and Dewilde, 1992), for convenience it is called CL-MOESP hereinafter. Practical usefulness has been demonstrated by several closed-loop system identification experiments (e.g. Oku and Ushida, 2009; Kojio et al., 2014; Nakayama and Oku, 2018). Asymptotic properties and optimality of CL-MOESP have been discussed by Oku (2010). Recently, Oku and Ikeda (2020) have studied the probability convergence property and the error analysis of the triangular matrix obtained from QR factorization.

In this paper, the limit value of the matrix to be singular-value decomposed will be investigated. The contribution is to prove the limit value of the matrix to be singular-value-decomposed has the dominant left singular vectors that span the subspace exactly equivalent to that spanned by the column vectors of the extended observability matrix of the system to be identified. It ensures that an estimate of the extended observability matrix obtained from CL-MOESP is consistent up to a similarity transform.

2. PROBLEM SETTING AND ASSUMPTIONS

Let us consider a closed-loop system depicted by Fig. 1. To simplify the problem, a constant gain feedback case is considered (Oku and Ikeda, 2020). Let $u_k, r_k \in \mathbb{R}^m$ denote the input and the external excitation signal, respectively. $y_k, e_k \in \mathbb{R}^l$ denote the output and noise, respectively. Suppose the signals, u_k, y_k and r_k are measurable, while e_k is not measurable. The set point is assumed to be $d_k \equiv 0$ for $\forall k$. Suppose that $\mathtt{P}$ to be identified is a n-th order linear time-invariant system of m inputs and l outputs with a minimal realization described by

$$x_{k+1} = Ax_k + Bu_k, \tag{1a}$$

$$y_k = Cx_k + e_k, \tag{1b}$$

where $x_k \in \mathbb{R}^n$ denotes the state vector of $\mathtt{P}$. Note that n is unknown. The input u_k is generated by subtraction of the output y_k multiplied by a constant feedback gain K from the external excitation signal r_k, that is,

$$u_k = r_k - Ky_k. \tag{2}$$

Through this paper, the following assumptions are made:

A1. The closed-loop system is internally stable, i.e., $|\lambda_i(\bar{A})| < 1$, where $\bar{A} := A - BKC$.

A2. The noise $\{e_k\}$ is an unknown discrete-time Gaussian process with the mean $\mathrm{E}[e_k] = 0$ and the covariance $\mathrm{E}[e_k e_\ell^\mathsf{T}] = \Omega_{ee}\delta_{k\ell}$, where $\mathrm{E}[\cdot]$ denotes the statistical expectation.

A3. The external excitation signal $\{r_k\}$ is a known discrete-time Gaussian process with the mean $\mathrm{E}[r_k] = 0$ and the covariance $\mathrm{E}[r_k r_\ell^\mathsf{T}] = \Omega_{rr}\delta_{k\ell}$. It persistently excites the closed-loop system appropriately.

A4. $\{r_k\}$ and $\{e_k\}$ are uncorrelated with each other in the sense that, for $\forall i, \forall j \in \mathbb{Z}$,

$$\lim_{M\to\infty} \frac{1}{M} \sum_{k=1}^{M} e_{i+k} r_{j+k}^\mathsf{T} = 0.$$

A5. For $\forall i \geq 0$, $\forall k$, x_k and r_{k+i} are independent of each other. So are x_k and e_{k+i}.

A6. The signals $\{x_k\}$, $\{r_k\}$, $\{u_k\}$, $\{y_k\}$ and $\{e_k\}$ are ergodic stationary processes.

⋆ This work was supported by JSPS KAKENHI Grant Number 18K04217.

Presented as late breaking results contribution
21st IFAC World Congress (Virtual)
Berlin, Germany, July 12-17, 2020

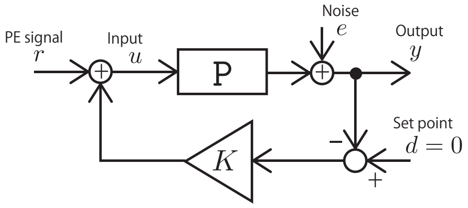

Fig. 1. A closed-loop system with constant gain feedback

3. NOTATIONS

The following notations are adopted: given i-successive sampled data of u from k, i.e., $\{u_k, \cdots, u_{k+i-1}\}$, define

$$u_i(k) := \left[\, u_k^\top \;\cdots\; u_{k+i-1}^\top \,\right]^\top. \tag{3}$$

Note that $r_i(k)$, $y_i(k)$ and $e_i(k)$ are also defined in a similar manner to (3).

Given a sequence $\{u_k\}$, the block Hankel matrix, $\mathcal{U}_{i,s,j} \in \mathbb{R}^{ms\times j}$, is defined as

$$\begin{aligned}\mathcal{U}_{i,s,j} &:= \begin{bmatrix} u_i & u_{i+1} & \cdots & u_{i+j-1} \\ u_{i+1} & u_{i+2} & \cdots & u_{i+j} \\ \vdots & \vdots & & \vdots \\ u_{i+s-1} & u_{i+s} & \cdots & u_{i+s+j-2} \end{bmatrix} \\ &= \left[\, u_s(i) \;\; u_s(i+1) \;\cdots\; u_s(i+j-1) \,\right],\end{aligned} \tag{4}$$

where the first subscript, i, is the same as the subscript on the top-left block element, and the others, s and j, mean that $\mathcal{U}_{i,s,j} \in \mathbb{R}^{ms\times j}$ is of s block rows and j columns. Note that $s > 0$ is a user-defined parameter which is chosen to be sufficiently larger than n. For sequences $\{y_k\}$, $\{r_k\}$ and $\{e_k\}$, the block Hankel matrices $\mathcal{Y}_{i,s,j}$, $\mathcal{R}_{i,s,j}$ and $\mathcal{E}_{i,s,j}$ are respectively defined in a manner similar to (4). These matrices are called the data Hankel matrices for the rest of this paper.

For brevity's sake, the following notations with respect to the data Hankel matrices are introduced: for an integer N that is sufficiently larger than s,

$$\begin{aligned}&\mathcal{R}_f := \mathcal{R}_{0,s,N}, \quad \mathcal{U}_f := \mathcal{U}_{0,s,N}, \quad \mathcal{E}_f := \mathcal{E}_{0,s,N}, \\ &\mathcal{R}_p := \mathcal{R}_{-s,s,N}, \quad \mathcal{U}_p := \mathcal{U}_{-s,s,N}, \quad \mathcal{E}_p := \mathcal{E}_{-s,s,N}, \\ &\mathcal{Y}_f := \mathcal{Y}_{0,s,N}, \quad \mathcal{R} := \left[\, \mathcal{R}_p^\top \; \mathcal{R}_f^\top \,\right]^\top, \quad \mathcal{E} := \left[\, \mathcal{E}_p^\top \; \mathcal{E}_f^\top \,\right]^\top.\end{aligned}$$

Note that the subscriptions "f" and "p" respectively represents that the data Hankel matrices are made of relatively "future" and "past" data, respectively.

For a sequence $\{x_k\}$, define

$$\mathcal{X}_{i,j} := \left[\, x_i \;\; x_{i+1} \;\cdots\; x_{i+j-1} \,\right], \tag{5}$$

and moreover define $\mathcal{X}_f := \mathcal{X}_{0,N}$ and $\mathcal{X}_p := \mathcal{X}_{-s,N}$.

Given a quadruple of matrices (E, F, G, H) of appropriate sizes, define the notations as follows (Ikeda, 2014):

$$\mathcal{O}_i(G,E) := \left[\, G^\top \; (GE)^\top \;\cdots\; (GE^{i-1})^\top \,\right]^\top, \tag{6}$$

$$\mathcal{L}_i(E,F) := \left[\, E^{i-1}F \;\cdots\; EF \;\; F \,\right], \tag{7}$$

$$\mathcal{T}_i(E,F,G,H) := \begin{bmatrix} H & & & 0 \\ GF & H & & \\ \vdots & \ddots & \ddots & \\ GE^{i-2}F & \cdots & GF & H \end{bmatrix}. \tag{8}$$

Especially, with respect to the system (1) to be identified, the extended observability matrix, the reversed extended controllability matrix and the block-Toeplitz matrix made of the Markov parameters, denoted briefly by $\mathcal{O}$, $\mathcal{L}$ and $\mathcal{T}$, respectively, are respectively defined as

$$\mathcal{O} := \mathcal{O}_s(C,A) \in \mathbb{R}^{ls\times n}, \qquad \mathcal{L} := \mathcal{L}_s(A,B) \in \mathbb{R}^{n\times ms},$$
$$\mathcal{T} := \mathcal{T}_s(A,B,C,0) \in \mathbb{R}^{ls\times ms}.$$

The covariance matrix of $\mathcal{R}_p$ as well as $\mathcal{R}_f$ is denoted by

$$\mathbf{\Omega}_{\mathcal{R}} := \lim_{N\to\infty} \frac{1}{N}\mathcal{R}_p\mathcal{R}_p^\top = \lim_{N\to\infty} \frac{1}{N}\mathcal{R}_f\mathcal{R}_f^\top = \begin{bmatrix} \Omega_{rr} & & 0 \\ & \ddots & \\ 0 & & \Omega_{rr} \end{bmatrix} \tag{9}$$

4. BRIEF REVIEW OF CL-MOESP

CL-MOESP is a solution to the following closed-loop subspace model identification problem.

Definition 1. Consider a closed-loop system depicted by Fig. 1. The problem is to estimate the order n of P to be identified and obtain the minimal realization $(A, B, C, 0)$ of (1) up to a similarity transform from the measurements of $\{r_k\}$, $\{u_k\}$ and $\{y_k\}$.

The procedure of CL-MOESP is as follows (Oku et al., 2006a,b):

Algorithm 1. (CL-MOESP). Suppose that a set of sampled data sequences $\{r_k\}$, $\{u_k\}$ and $\{y_k\}$ be obtained from a system identification experiment of the closed-loop system as depicted in Fig. 1. Then, a state-space model which represents the input/output relation of P can be obtained according to the procedures as follows:

1. Execute the QR factorization of the following matrix:
$$\begin{bmatrix} \mathcal{R} \\ \mathcal{U}_p \\ \mathcal{U}_f \\ \mathcal{Y}_f \end{bmatrix} = \begin{bmatrix} L_{11} & & & \\ L_{21} & L_{22} & & \\ L_{31} & L_{32} & L_{33} & \\ L_{41} & L_{42} & L_{43} & L_{44} \end{bmatrix} \begin{bmatrix} Q_1^\top \\ Q_2^\top \\ Q_3^\top \\ Q_4^\top \end{bmatrix} \tag{10}$$
2. Compute P and $\Upsilon^{\frac{1}{2}}$ as follows:
$$P := L_{21} - L_{21}L_{31}^\top \left(L_{31}L_{31}^\top\right)^{-1} L_{31} \tag{11}$$
$$\Upsilon^{\frac{1}{2}} := L_{41}P^\top \left(PP^\top\right)^{-\frac{1}{2}}. \tag{12}$$
3. To estimate the extended observability matrix, $\mathcal{O}$, up to a similarity transform, execute singular value decomposition (SVD) of $\Upsilon^{\frac{1}{2}}$ and we have
$$\Upsilon^{\frac{1}{2}} = \left[\, \hat{U} \;\; \hat{U}^\perp \,\right] \begin{bmatrix} \hat{\Sigma} & \\ & \hat{\Sigma}^\perp \end{bmatrix} \begin{bmatrix} \hat{V}^\top \\ \left(\hat{V}^\perp\right)^\top \end{bmatrix}, \tag{13}$$
where the diagonal matrix $\hat{\Sigma} \in \mathbb{R}^{n\times n}$ has n dominant singular values as its diagonal entries. Namely, the number of the dominant singular values can estimate the order of P. Note that the orthogonal matrix $\hat{U}$ is an estimate of $\mathcal{O}$ up to a similarity transform.
4. The set of estimates of the coefficients of a state-space representation of P, i.e., $(\hat{A}, \hat{B}, \hat{C}, \hat{D})$, can be obtained according to the procedure similar in the paper of Verhaegen and Dewilde (1992).

Presented as late breaking results contribution
21st IFAC World Congress (Virtual)
Berlin, Germany, July 12-17, 2020

5. DERIVATION OF THE MATRIX I/O EQUATIONS

Substitution of (2) into (1a) yields

$$x_{k+1} = \bar{A}x_k + Br_k + B_e e_k, \tag{14}$$

where $B_e := -BK$. Recursive use of (14) gives, for $i \geq 1$,

$$x_{k+i} = \bar{A}^i x_k + \mathcal{L}_i(\bar{A}, B)r_i(k) + \mathcal{L}_i(\bar{A}, B_e)e_i(k). \tag{15}$$

For an integer s sufficiently greater than n, Using the output equation (1b) and (15),

$$\begin{aligned} y_{k+i} = {} & C\bar{A}^i x_k + C\mathcal{L}_i(\bar{A}, B)r_i(k) \\ & + C\mathcal{L}_i(\bar{A}, B_e)e_i(k) + e_{k+i} \end{aligned} \tag{16}$$

is derived for $i = 0, \cdots, s-1$. Then, stack (16) for $i = 0, \cdots, s-1$, and we have the following equation:

$$y_s(k) = \mathcal{O}_y x_k + \mathcal{T}_y r_s(k) + \mathcal{H}_y e_s(k), \tag{17}$$

where $\mathcal{H}_y := \mathcal{T}_s(\bar{A}, B_e, C, I)$,

$$\mathcal{O}_y := \mathcal{O}_s(C, \bar{A}), \qquad \mathcal{T}_y := \mathcal{T}_s(\bar{A}, B, C, 0). \tag{18}$$

Moreover, place (17) for $k = 0, \cdots, N$ side by side, and we obtain the following matrix input-output equation:

$$\mathcal{Y}_f = \mathcal{O}_y \mathcal{X}_f + \mathcal{T}_y \mathcal{R}_f + \mathcal{H}_y \mathcal{E}_f. \tag{19}$$

Follow the same path as mentioned above, and we have the following equation with respect to $u_s(k)$:

$$u_s(k) = \mathcal{O}_u x_k + \mathcal{T}_u r_s(k) + \mathcal{H}_u e_s(k) \tag{20}$$

where $H := -KC$, $\mathcal{H}_u := \mathcal{T}_s(\bar{A}, B_e, H, -K)$,

$$\mathcal{O}_u := \mathcal{O}_s(H, \bar{A}), \qquad \mathcal{T}_u = \mathcal{T}_s(\bar{A}, B, H, I). \tag{21}$$

Then, place (20) for $k = 0, \cdots, N$ side by side, and we derive the following matrix input-output equation:

$$\mathcal{U}_f = \mathcal{O}_u \mathcal{X}_f + \mathcal{T}_u \mathcal{R}_f + \mathcal{H}_u \mathcal{E}_f. \tag{22}$$

Now, let us get back to (15) for $i = s$. Replace k in (15) by $k - s$ and we have

$$x_k = \bar{A}^s x_{k-s} + \mathcal{L}_r r_s(k-s) + \mathcal{L}_e e_s(k-s), \tag{23}$$

where $\mathcal{L}_r := \mathcal{L}_s(\bar{A}, B)$ and $\mathcal{L}_e := \mathcal{L}_s(\bar{A}, B_e)$. Then, place (23) for $k = 0, \cdots, N$ side by side, and we have the s-step ahead matrix state equation as follows:

$$\mathcal{X}_f = \bar{A}^s \mathcal{X}_p + \mathcal{L}_r \mathcal{R}_p + \mathcal{L}_e \mathcal{E}_p \tag{24}$$

Finally, substitute (19) and (22) into (24) and notice an analogy between $\mathcal{U}_p$ and $\mathcal{U}_f$ with respect to (22), and we have the following matrix input-output equations:

$$\begin{aligned} \begin{bmatrix} \mathcal{U}_p \\ \mathcal{U}_f \\ \mathcal{Y}_f \end{bmatrix} = {} & \begin{bmatrix} \mathcal{O}_u \\ \mathcal{O}_u \bar{A}^s \\ \mathcal{O}_y \bar{A}^s \end{bmatrix} \mathcal{X}_p + \begin{bmatrix} \mathcal{T}_u & 0 \\ \mathcal{O}_u \mathcal{L}_r & \mathcal{T}_u \\ \mathcal{O}_y \mathcal{L}_r & \mathcal{T}_y \end{bmatrix} \mathcal{R} \\ & + \begin{bmatrix} \mathcal{H}_u & 0 \\ \mathcal{O}_u \mathcal{L}_e & \mathcal{H}_u \\ \mathcal{O}_y \mathcal{L}_e & \mathcal{H}_y \end{bmatrix} \mathcal{E} \end{aligned} \tag{25}$$

6. ON ASYMPTOTIC PROPERTIES OF L MATRIX

Oku and Ikeda (2020) have studied error analysis of the triangular matrix obtained from the QR factorization (10). Especially, since (10), (11) and (12) imply that the matrix with 3 block entries

$$\begin{bmatrix} L_{21}^\mathsf{T} & L_{31}^\mathsf{T} & L_{41}^\mathsf{T} \end{bmatrix}^\mathsf{T} \tag{26}$$

plays a key role in derivation of $\Upsilon^{\frac{1}{2}}$ and the subsequent procedures of CL-MOESP, they have investigated convergence properties and the error covariance of (26). This section is dedicated to introducing the results of Oku and Ikeda (2020) used here.

Lemma 2. Assume that the matrix $\mathcal{R}$ is of full row rank. Then, it holds that

$$\begin{bmatrix} L_{21} \\ L_{31} \\ L_{41} \end{bmatrix} = \begin{bmatrix} \mathcal{U}_p \\ \mathcal{U}_f \\ \mathcal{Y}_f \end{bmatrix} \mathcal{R}^\mathsf{T} L_{11}^{-\mathsf{T}} \tag{27}$$

Substitution of (25) into (27) with some calculations brings us to

$$\begin{bmatrix} L_{21} \\ L_{31} \\ L_{41} \end{bmatrix} = \mathcal{S}_N + \mathcal{N}_N, \tag{28}$$

where the signal-based component, $\mathcal{S}_N$, and the noise-based component, $\mathcal{N}_N$, of (28), are given respectively as follows:

$$\mathcal{S}_N := \begin{bmatrix} \mathcal{O}_u \\ \mathcal{O}_u \bar{A}^s \\ \mathcal{O}_y \bar{A}^s \end{bmatrix} \mathcal{X}_p \mathcal{R}^\mathsf{T} L_{11}^{-\mathsf{T}} + \begin{bmatrix} \mathcal{T}_u & 0 \\ \mathcal{O}_u \mathcal{L}_r & \mathcal{T}_u \\ \mathcal{O}_y \mathcal{L}_r & \mathcal{T}_y \end{bmatrix} L_{11},$$

$$\mathcal{N}_N := \begin{bmatrix} \mathcal{H}_u & 0 \\ \mathcal{O}_u \mathcal{L}_e & \mathcal{H}_u \\ \mathcal{O}_y \mathcal{L}_e & \mathcal{H}_y \end{bmatrix} \mathcal{E} \mathcal{R}^\mathsf{T} L_{11}^{-\mathsf{T}}.$$

The lower triangular matrix $\bar{\boldsymbol{L}}_{11}$ is defined as the Cholesky factor, up to a sign matrix, of the following asymptotic covariance matrix:

$$\bar{\boldsymbol{L}}_{11} \bar{\boldsymbol{L}}_{11}^\mathsf{T} := \lim_{N \to \infty} \frac{1}{N} \mathcal{R}\mathcal{R}^\mathsf{T} = \begin{bmatrix} \boldsymbol{\Omega}_\mathcal{R} & 0 \\ 0 & \boldsymbol{\Omega}_\mathcal{R} \end{bmatrix}. \tag{29}$$

Notice that the off-diagonal block elements are null since, due to A3, $\lim_{N \to \infty} \frac{1}{N} \mathcal{R}_p \mathcal{R}_f^\mathsf{T} = 0$. Hereafter, let us assume that the sign matrix is determined compatibly with the context.

The following theorem is for the probability convergence property of the signal-based component $\mathcal{S}_N$:

Theorem 3. (Oku and Ikeda, 2020) Under the assumptions from A1 to A6,

$$\operatorname*{plim}_{N \to \infty} \frac{1}{\sqrt{N}} \mathcal{S}_N = \begin{bmatrix} \mathcal{T}_u & 0 \\ \mathcal{O}_u \mathcal{L}_r & \mathcal{T}_u \\ \mathcal{O}_y \mathcal{L}_r & \mathcal{T}_y \end{bmatrix} \bar{\boldsymbol{L}}_{11} =: \mathcal{S}_\infty.$$

Proof. Note that from the assumption **A5** the following uncorrelation property holds:

$$\lim_{N \to \infty} \frac{1}{N} \mathcal{X}_p \mathcal{R}^\mathsf{T} = 0.$$

For $\forall \varepsilon > 0$, as $N \to \infty$,

$$\begin{aligned} & \mathrm{P}\left[\left\| \frac{1}{\sqrt{N}} \mathcal{S}_N - \mathcal{S}_\infty \right\|_F > \varepsilon \right] \\ & \leq \mathrm{P}\left[\left\| \begin{bmatrix} \mathcal{O}_u \\ \mathcal{O}_u \bar{A}^s \\ \mathcal{O}_y \bar{A}^s \end{bmatrix} \frac{1}{N} \mathcal{X}_p \mathcal{R}^\mathsf{T} \left(\frac{1}{\sqrt{N}} L_{11} \right)^{-\mathsf{T}} \right\|_F \right. \\ & \qquad \left. + \left\| \begin{bmatrix} \mathcal{T}_u & 0 \\ \mathcal{O}_u \mathcal{L}_r & \mathcal{T}_u \\ \mathcal{O}_y \mathcal{L}_r & \mathcal{T}_y \end{bmatrix} \left(\frac{1}{\sqrt{N}} L_{11} - \bar{\boldsymbol{L}}_{11} \right) \right\|_F > \varepsilon \right] \\ & \longrightarrow 0, \end{aligned}$$

where $\| \cdot \|_F$ denotes the Frobenius norm. □

The following theorem is for the probability convergence property of the noise-based component $\mathcal{N}_N$:

Theorem 4. (Oku and Ikeda, 2020) Under the assumptions from A1 to A6,

$$\operatorname*{plim}_{N\to\infty}\frac{1}{\sqrt{N}}\mathcal{N}_N=0. \tag{30}$$

Proof. The assumption **A4** gives

$$\lim_{N\to\infty}\frac{1}{N}\mathcal{E}\mathcal{R}^\mathsf{T}=0.$$

Then, for $\forall\varepsilon>0$, it holds that

$$\lim_{N\to 0}\mathrm{P}\left[\left\|\begin{bmatrix}\mathcal{H}_u & 0\\ \mathcal{O}_u\mathcal{L}_e & \mathcal{H}_u\\ \mathcal{O}_y\mathcal{L}_e & \mathcal{H}_y\end{bmatrix}\frac{1}{N}\mathcal{E}\mathcal{R}^\mathsf{T}\left(\frac{1}{\sqrt{N}}L_{11}\right)^{-\mathsf{T}}\right\|_F\geq\varepsilon\right]=0$$

□

Corollary 5. The limit values of 3 block entries in (26) are given by

$$\begin{bmatrix}\bar{\boldsymbol{L}}_{21}\\ \bar{\boldsymbol{L}}_{31}\\ \bar{\boldsymbol{L}}_{41}\end{bmatrix}:=\operatorname*{plim}_{N\to\infty}\frac{1}{\sqrt{N}}\begin{bmatrix}L_{21}\\ L_{31}\\ L_{41}\end{bmatrix}=\begin{bmatrix}\mathcal{T}_u & 0\\ \mathcal{O}_u\mathcal{L}_r & \mathcal{T}_u\\ \mathcal{O}_y\mathcal{L}_r & \mathcal{T}_y\end{bmatrix}\bar{\boldsymbol{L}}_{11}. \tag{31}$$

Proof. It is obvious from A5, (28), Theorems 3 and 4. □

7. MAIN RESULT

Since from (13) the dominant left singular vectors of $\Upsilon^{\frac{1}{2}}$ is crucially important to estimate the extended observability matrix $\mathcal{O}$, the limit value of $\Upsilon^{\frac{1}{2}}$, or equivalently, the limit value of Υ, i.e.,

$$\bar{\boldsymbol{\Upsilon}}:=\operatorname*{plim}_{N\to\infty}\frac{1}{N}\Upsilon=\operatorname*{plim}_{N\to\infty}\frac{1}{N}\Upsilon^{\frac{1}{2}}\left(\Upsilon^{\frac{1}{2}}\right)^\mathsf{T} \tag{32}$$

is the center of interest in this paper.

The limit values of (11) can be calculated as

$$\begin{aligned}\bar{\boldsymbol{P}}&:=\operatorname*{plim}_{N\to\infty}\frac{1}{\sqrt{N}}P\\ &=\operatorname*{plim}_{N\to\infty}\left(\frac{1}{\sqrt{N}}L_{21}\right.\\ &\qquad\left.-\left(\frac{1}{N}L_{21}L_{31}^\mathsf{T}\right)\left(\frac{1}{N}L_{31}L_{31}^\mathsf{T}\right)^{-1}\frac{1}{\sqrt{N}}L_{31}\right)\\ &=\bar{\boldsymbol{L}}_{21}-\bar{\boldsymbol{L}}_{21}\bar{\boldsymbol{L}}_{31}^\mathsf{T}\left(\bar{\boldsymbol{L}}_{31}\bar{\boldsymbol{L}}_{31}^\mathsf{T}\right)^{-1}\bar{\boldsymbol{L}}_{31}.\end{aligned} \tag{33}$$

The following theorem is the main result of this paper.

Theorem 6. The limit of Υ is given as follows:

$$\bar{\boldsymbol{\Upsilon}}=\mathcal{O}\mathcal{L}\left(\bar{\boldsymbol{P}}\bar{\boldsymbol{P}}^\mathsf{T}\right)\mathcal{L}^\mathsf{T}\mathcal{O}^\mathsf{T}.$$

Proof. A complete proof requires tediously long calculation. A sketch of proof is provided here.

Substitute (12) into (32) and take the limit as N goes to infinity, and we have

$$\bar{\boldsymbol{\Upsilon}}=\left(\bar{\boldsymbol{L}}_{41}\bar{\boldsymbol{P}}^\mathsf{T}\right)\left(\bar{\boldsymbol{P}}\bar{\boldsymbol{P}}^\mathsf{T}\right)^{-1}\left(\bar{\boldsymbol{L}}_{41}\bar{\boldsymbol{P}}^\mathsf{T}\right)^\mathsf{T} \tag{34}$$

Then, we will calculate the two terms, $\bar{\boldsymbol{L}}_{41}\bar{\boldsymbol{P}}^\mathsf{T}$ and $\bar{\boldsymbol{P}}\bar{\boldsymbol{P}}^\mathsf{T}$ in (34). Substitution of (31) into (33) with some calculation brings us to

$$\begin{aligned}\bar{\boldsymbol{P}}\bar{\boldsymbol{P}}^\mathsf{T}&=\mathcal{T}_u\boldsymbol{\Omega}_\mathcal{R}\left(\boldsymbol{\Omega}_\mathcal{R}^{-1}-\mathcal{L}_r^\mathsf{T}\mathcal{O}_u^\mathsf{T}\right.\\ &\quad\cdot\left.\left(\mathcal{O}_u\mathcal{L}_r\boldsymbol{\Omega}_\mathcal{R}\mathcal{L}_r^\mathsf{T}\mathcal{O}_u^\mathsf{T}+\mathcal{T}_u\boldsymbol{\Omega}_\mathcal{R}\mathcal{T}_u^\mathsf{T}\right)^{-1}\mathcal{O}_u\mathcal{L}_r\right)\boldsymbol{\Omega}_\mathcal{R}\mathcal{T}_u^\mathsf{T},\end{aligned} \tag{35}$$

and moreover,

$$\bar{\boldsymbol{L}}_{41}\bar{\boldsymbol{P}}^\mathsf{T}=\left(\mathcal{O}_y-\mathcal{T}_y\mathcal{T}_u^{-1}\mathcal{O}_u\right)\mathcal{L}_r\mathcal{T}_u^{-1}\bar{\boldsymbol{P}}\bar{\boldsymbol{P}}^\mathsf{T}. \tag{36}$$

Note the invertibility of $\mathcal{T}_u=\mathcal{T}_s(\bar{A},B,H,I)$. Note also that the assumption A3 means the invertibility of (35). Substitution of (35) and (36) into (34) yields

$$\begin{aligned}\bar{\boldsymbol{\Upsilon}}&=\left(\mathcal{O}_y-\mathcal{T}_y\mathcal{T}_u^{-1}\mathcal{O}_u\right)\mathcal{L}_r\mathcal{T}_u^{-1}\bar{\boldsymbol{P}}\bar{\boldsymbol{P}}^\mathsf{T}\\ &\quad\cdot\mathcal{T}_u^{-\mathsf{T}}\mathcal{L}_r^\mathsf{T}\left(\mathcal{O}_y-\mathcal{T}_y\mathcal{T}_u^{-1}\mathcal{O}_u\right)^\mathsf{T}\end{aligned} \tag{37}$$

Now, note again that $\mathcal{T}_u$ is invertible and actually,

$$\mathcal{T}_u^{-1}=\mathcal{T}_s(\bar{A}-BH,B,-H,I)=\mathcal{T}_s(A,B,-H,I). \tag{38}$$

Then, keeping the definitions of notations (6), (7), (8), (18) and (21) in mind, two terms, $\mathcal{O}_y-\mathcal{T}_y\mathcal{T}_u^{-1}\mathcal{O}_u$ and $\mathcal{L}_r\mathcal{T}_u^{-1}$, in (37) can be calculated as

$$\begin{aligned}\mathcal{O}_y-\mathcal{T}_y\mathcal{T}_u^{-1}\mathcal{O}_u&=\mathcal{O}_s(C,\bar{A}-BH)=\mathcal{O}_s(C,A)=\mathcal{O},\\ \mathcal{L}_r\mathcal{T}_u^{-1}&=\mathcal{L}_s(\bar{A}-BH,B)=\mathcal{L}_s(A,B)=\mathcal{L}.\end{aligned}$$

Hence, this concludes the sketch of proof. □

Theorem 6 implies that the dominant left singular vectors of $\bar{\boldsymbol{\Upsilon}}$ span the subspace exactly equivalent to the subspace spanned by the column vectors of the extended observability matrix $\mathcal{O}$ of the system (1) to be identified. It confirms that CL-MOESP(Oku et al., 2006a,b) gives a consistent estimate, up to a similarity transform, of the extended observability matrix $\hat{U}$ via the singular value decomposition of $\Upsilon^{\frac{1}{2}}$ of (13).

REFERENCES

Chiuso, A. (2006). Asymptotic Variance of Closed-Loop Subspace Identification Methods. *IEEE Trans. on Automatic Control*, 51(8), 1299–1314.

Chiuso, A. (2010). On the Asymptotic Properties of Closed-Loop CCA-Type Subspace Algorithm. *IEEE Trans. on Automatic Control*, 55(3), 634–649.

Chiuso, A. and Picci, G. (2005). Consistency Analysis of Certain Closed-Loop Subspace Identification Methods. *Automatica*, 41(3), 377–391.

Ikeda, K. (2014). On the precision of the plant estimates in some subspace identification methods. In *Proceedings of the 19th IFAC World Congress*, 9516–9521. Cape Town.

Kojio, J., Ishibashi, H., Inoue, R., Ushida, S., and Oku, H. (2014). MIMO Closed-loop Subspace Model Identification and Hovering Control of a 6-DOF Coaxial Miniature Helicopter. In *Proceedings of SICE Annual Conference 2014*, 1679–1684. Sapporo.

Nakayama, M. and Oku, H. (2018). An Experiment on Closed-loop System Identification of UAV Using Dual-rate Sampling. In *Proceedings of the 18th IFAC Symposium on System Identification*, 598–603. Stockholm.

Oku, H. (2010). On asymptotic properties of MOESP-type closed-loop subspace model identification. In *Proceedings of MTNS 2010*, 1015–1022. Kyoto, Japan.

Oku, H., Ogura, Y., and Fujii, T. (2006a). Closed-Loop Subspace Model Identification Based on QR-Factorization. In *Proceedings of MTNS 2006*, 385–390. Kyoto, Japan.

Oku, H., Ogura, Y., and Fujii, T. (2006b). MOESP-type Closed-loop Subspace Model Identification Method. *Trans. of the Society of Instrument and Control Engineers*, 42(6), 636–642.

Oku, H. and Ikeda, K. (2020). On error analysis of a closed-loop subspace model identification method. In *the paper submitted to 24th International Symposium on Mathematical Theory of Networks and Systems.*

Oku, H. and Ushida, S. (2009). Experiment on closed-loop subspace model identification of an unstable underactuated system. In *Proceedings of ICCAS-SICE 2009*, 4902–4907. Fukuoka.

Verhaegen, M. and Dewilde, P. (1992). Subspace model identification Part I: The output-error state space model identification class of algorithms. *Int. J. Control*, 56(5), 1187–1210.